Batf coordinates multiple aspects of B and T cell function required for normal antibody responses

Briana C. Betz,[1] Kimberly L. Jordan-Williams,[1] Chuanwu Wang,[2] Seung Goo Kang,[2] Juan Liao,[1] Michael R. Logan,[2] Chang H. Kim,[2,3] and Elizabeth J. Taparowsky[1,3]

[1]Department of Biological Sciences, [2]Department of Comparative Pathobiology and [3]Purdue University Center for Cancer Research, Purdue University West Lafayette, IN 47907

Batf belongs to the activator protein 1 superfamily of basic leucine zipper transcription factors that includes Fos, Jun, and Atf proteins. Batf is expressed in mouse T and B lymphocytes, although the importance of Batf to the function of these lineages has not been fully investigated. We generated mice (*Batf*$^{\Delta Z/\Delta Z}$) in which Batf protein is not produced. *Batf*$^{\Delta Z/\Delta Z}$ mice contain normal numbers of B cells but show reduced numbers of peripheral CD4$^+$ T cells. Analysis of CD4$^+$ T helper (Th) cell subsets in *Batf*$^{\Delta Z/\Delta Z}$ mice demonstrated that Batf is required for the development of functional Th type 17 (Th17), Th2, and follicular Th (Tfh) cells. In response to antigen immunization, germinal centers were absent in *Batf*$^{\Delta Z/\Delta Z}$ mice and the maturation of Ig-secreting B cells was impaired. Although adoptive transfer experiments confirmed that this B cell phenotype can be driven by defects in the *Batf*$^{\Delta Z/\Delta Z}$ CD4$^+$ T cell compartment, stimulation of *Batf*$^{\Delta Z/\Delta Z}$ B cells in vitro, or by a T cell–independent antigen in vivo, resulted in proliferation but not class-switch recombination. We conclude that loss of Batf disrupts multiple components of the lymphocyte communication network that are required for a robust immune response.

CORRESPONDENCE
Elizabeth J. Taparowsky:
taparows@purdue.edu

Abbreviations used: Ab, antibody; AP-1, activator protein 1; bZIP, basic leucine zipper; CSR, class-switch recombination; GC, germinal center; HA, hemagglutinin antigen; IHC, immunohistochemistry; PNA, peanut agglutinin; PP, Peyer's patch; qPCR, quantitative PCR; sRBC, sheep RBC; Tfh, follicular Th cell; T reg cell, regulatory T cell.

The development of the various lymphoid lineages is regulated by many transcription factors, including the dimerizing basic leucine zipper (bZIP) proteins collectively known as activator protein 1 (AP-1; Wagner and Eferl, 2005). The classical AP-1 transcription factor consists of a Jun:Fos heterodimer, although tissue-restricted bZIP proteins, including several of the Maf, Atf, and Batf proteins, provide alternative partner choices for Fos and/or Jun (Eferl and Wagner, 2003). Properties conferred on AP-1 by dimer composition and posttranslational modifications influence the DNA targets bound by AP-1 and, in some cases, convert what is normally a transcriptional activator into a transcriptional repressor (Eferl and Wagner, 2003; Hess et al., 2004; Amoutzias et al., 2006). It is not surprising, therefore, that AP-1 plays roles in cell growth, differentiation, and apoptosis (Hess et al., 2004) and that deregulated AP-1 activity is a feature of many pathologies, including cancer and neurological diseases (Eferl and Wagner, 2003; Raivich and Behrens, 2006).

Our laboratory studies Batf, an AP-1 protein which is expressed in immune cells and whose overall level of expression is regulated by developmental transitions (Li et al., 2001; Williams et al., 2001) and environmental cues (Senga et al., 2002; Johansen et al., 2003; Jung et al., 2004). Batf is the founding member of the Batf protein family (Batf, Batf2, and Batf3; Dorsey et al., 1995; Aronheim et al., 1997; Lim et al., 2006). All three Batf proteins compete with Fos for partnering with Jun and, in doing so, generate bZIP dimers that inhibit the transcription of AP-1 reporter genes (Echlin et al., 2000; Iacobelli et al., 2000; Su et al., 2008). Previous studies using a thymus-specific *BATF* transgene examined how constitutive AP-1 inhibition has an impact on the growth and development of T cells in vivo. Results showed that although the proliferative response

The Rockefeller University Press $30.00
J. Exp. Med. Vol. 207 No. 5 933-942
www.jem.org/cgi/doi/10.1084/jem.20091548

The Journal of Experimental Medicine

of transgenic thymocytes was decreased in vitro, all T cell subsets, with the exception of NKT cells, were present in normal numbers in vivo (Williams et al., 2003; Zullo et al., 2007). The exquisite sensitivity of Vαi NKT cells to *BATF* overexpression provided the first evidence that downstream signaling through the invariant NKT cell receptor, which is largely responsible for the unique properties of these cells (Kronenberg and Engel, 2007), relies on the precise regulation of AP-1.

In this study, we report the immune system phenotype of mice ($Batf^{\Delta Z/\Delta Z}$) in which Batf protein expression has been eliminated. In these animals, the numbers of peripheral T cells, but not B cells, are affected. In agreement with a study published while this work was in progress (Schraml et al., 2009), we detect a significant decrease in $CD4^+$ T cells and a dramatic reduction in Th17 cells. However, we also report that loss of Batf has a negative impact on Th2 cells, follicular Th (Tfh) cells, and the humoral immune response. Germinal centers (GCs) do not form in antigen-challenged $Batf^{\Delta Z/\Delta Z}$ mice and B cells do not undergo productive Ig class-switch recombination (CSR), leading to dysgammaglobulinemia. These data identify essential roles for Batf in several Th cell lineages and in coordinating the transcriptional program required for the differentiation of peripheral B cells into antibody (Ab)-producing cells.

RESULTS AND DISCUSSION

Decreased numbers of peripheral $CD4^+$ T cells in $Batf^{\Delta Z/\Delta Z}$ mice

To examine the role of Batf in lymphocyte development, we first generated *Batf* knockin (*Batf KI*) mice in which exon 3, the ZIP coding region of *Batf*, is expressed with a C-terminal hemagglutinin antigen (HA) epitope tag (Fig. 1 A). This modified exon and the *Pgk-neo* cassette used for ES cell selection are flanked by *loxP* sites, permitting the excision of both elements using Cre recombinase. *Batf KI* mice were crossed to Cre-expressing mice (*EIIa-Cre*), producing heterozygous ($Batf^{+/\Delta Z}$) mice which were crossed to generate homozygous $Batf^{\Delta Z/\Delta Z}$ mice and littermate $Batf^{+/\Delta Z}$ and $Batf^{+/+}$ mice for comparison (Fig. 1, A and B). $Batf^{\Delta Z/\Delta Z}$ mice do not produce a functional Batf bZIP protein. Immunoblots using $Batf^{\Delta Z/\Delta Z}$ splenocyte extracts and anti-HA antiserum failed to detect a protein (Fig. 1 C). As predicted, semi-quantitative PCR (qPCR) analysis of RNA isolated from $Batf^{\Delta Z/\Delta Z}$ splenocytes using several primer sets detected transcripts representing exons 1 and 2 but no transcript specifying the Batf ZIP domain (Fig. S1, A and B).

Batf mRNA and protein are expressed in mouse B cells and in all major T cell subsets examined, with the exception of double-positive thymocytes (Williams et al., 2001) which, interestingly, lack all AP-1 activity (Rincón and Flavell, 1996). Mice expressing human BATF throughout T cell development in the thymus ($p56^{lck}$*HA-BATF*) possess normal numbers of $CD4^+$ and $CD8^+$ T cells but are impaired in the development of Vαi NKT cells (Williams et al., 2003; Zullo et al., 2007). To determine if B or T cell development is altered by the absence of Batf, cells from the thymus, spleen, and Peyer's patches (PPs) of $Batf^{+/+}$ and $Batf^{\Delta Z/\Delta Z}$ mice were analyzed by flow cytometry. No significant difference in thymic T cell populations was observed (Fig. S2 A). In the periphery, a trend toward a decreased number of T cells and an increase in B cell numbers was noted, yet statistical significance was established only for $CD4^+$ T cells (Fig. 1 D). In agreement with a recent study (Schraml et al., 2009), we did not detect increases in any T cell subset in $Batf^{\Delta Z/\Delta Z}$ mice, including Vαi NKT cells (unpublished data). This was unexpected based on the NKT cell–deficient phenotype of $p56^{lck}$*HA-BATF* mice (Williams et al., 2001; Zullo et al., 2007) and on experimental evidence that BATF inhibits cell proliferation in several different contexts (Echlin et al., 2000; Williams et al., 2001; Senga et al., 2002; Thornton et al., 2006). Instead, this supports a model where the overexpression of an AP-1 inhibitor, such as Batf, can have a dramatic impact on cells, whereas the impact of deleting Batf might be masked by the compensatory actions of other AP-1 inhibitors (e.g., Batf3, JunD, FosB, and Atf3; Hess et al., 2004). Although a comparative profile of all AP-1 proteins expressed by various lymphocyte lineages has yet to be compiled, Batf and Batf3 are coexpressed in mouse Th1 cells, for example (Williams et al., 2001; Hildner et al., 2008). In this regard, transgenic mice in which either of these proteins is overexpressed during T cell development share phenotypes, including the NKT cell defect (unpublished data), whereas the absence of Batf or Batf3 has an impact on other cell types (Hildner et al., 2008; Schraml et al., 2009). Thus, it is the unique functions of Batf that will be revealed by a thorough analysis of $Batf^{\Delta Z/\Delta Z}$ mice.

Th2 and Th17 cells require Batf

The decrease in peripheral $CD4^+$ T cells associated with Batf deficiency prompted us to further investigate this phenotype. $CD4^+$ T cells represent multiple T helper (Th) cell lineages (Zhou et al., 2009). To measure Th cell subsets in $Batf^{+/+}$ and $Batf^{\Delta Z/\Delta Z}$ mice, $CD4^+$ T cells isolated directly from spleen and PP were analyzed by flow cytometry after a brief stimulation. IFN-γ and IL-4 are well characterized markers of the Th1 and Th2 lineages, respectively, and no statistically significant difference was noted for either cell type (Fig. 2 A). In contrast, a dramatic underrepresentation of $CD4^+$ T cells expressing IL-17 (Th17 cells) was apparent in $Batf^{\Delta Z/\Delta Z}$ mice (Fig. 2 A). A small but significant reduction in $Foxp3^+$ $CD4^+$ regulatory T (T reg) cells also was noted in $Batf^{\Delta Z/\Delta Z}$ mice (Fig. S2 B).

To investigate if Batf deficiency affects the expression of genes that are markers for activated $CD4^+$ Th cell subsets, RNA was prepared from $CD4^+$ $Batf^{+/+}$ and $Batf^{\Delta Z/\Delta Z}$ splenocytes after stimulation with anti-CD3ε mAb for 48 h. qPCR was used to quantify transcripts unique to Th17 (*IL-21*, *IL-23R*, and *IL-17*), Th1 (*T-bet*), Th2 (*Gata3* and *IL-4*), and T reg (*Foxp3*) cells. Results confirm the underrepresentation of Th17 cells, the normal levels of Th1 cells, and the modest reduction of T reg cells in $Batf^{\Delta Z/\Delta Z}$ mice (Fig. 2 B). Interestingly, although no significant change in Th2 cells was detected by flow cytometry (Fig. 2 A), the low levels of

IL-4 and *Gata3* mRNA noted in Fig. 2 B suggest a role for Batf in Th2 responses. As confirmation that a difference in mRNA by this assay reflects a change in protein, ELISA was performed on media harvested from stimulated $Batf^{+/+}$ and $Batf^{\Delta Z/\Delta Z}$ splenocytes. Results showed that $Batf^{\Delta Z/\Delta Z}$ cells secrete normal levels of IFN-γ, reduced levels of IL-4, and extremely low levels of IL-17 (unpublished data).

To compare the ability of $Batf^{+/+}$ and $Batf^{\Delta Z/\Delta Z}$ $CD4^+$ T cells to respond to cues that polarize cells to distinct Th cell lineages, naive $CD4^+$ T splenocytes, cultured under well defined Th1, Th2, Th17, and T reg cell conditions, were analyzed by flow cytometry. This general approach was used previously (Schraml et al. 2009) to demonstrate a role for Batf in Th17 differentiation. In agreement with those studies, we found that $Batf^{+/+}$ and $Batf^{\Delta Z/\Delta Z}$ cells were equally competent for Th1 differentiation (Fig. S2 C) and that the decreased levels of T reg cells noted in vivo did not reflect an inability of naive $Batf^{\Delta Z/\Delta Z}$ T cells to differentiate to T reg cells in vitro (Fig. S2 D). Our results also confirmed that $Batf^{\Delta Z/\Delta Z}$ cells cannot be directed toward the Th17 lineage under conditions where >40% of control $Batf^{+/+}$ cells express IL-17 (Fig. S2 E). In contrast, attempts to assess Th2 polarization by flow cytometry produced inconsistent results for both $Batf^{+/+}$ and $Batf^{\Delta Z/\Delta Z}$ cells over several experiments, prompting us to rely on qPCR analysis of Th2 transcripts as an indicator of differentiation. qPCR with RNA from in vitro–polarized Th17 cultures was performed in parallel. As shown in Fig. 2 (C and D), when compared with control cells, $Batf^{\Delta Z/\Delta Z}$ cells did not induce significant levels of either Th2- or Th17-specific transcripts. Although Schraml et al. (2009) did not describe a defect in polarized Th2 differentiation for their Batf-deficient cells, our results would indicate that there is, at minimum, a partial defect in the Th2 cell subset that contributes to a decreased level of IL-4 in $Batf^{\Delta Z/\Delta Z}$ mice.

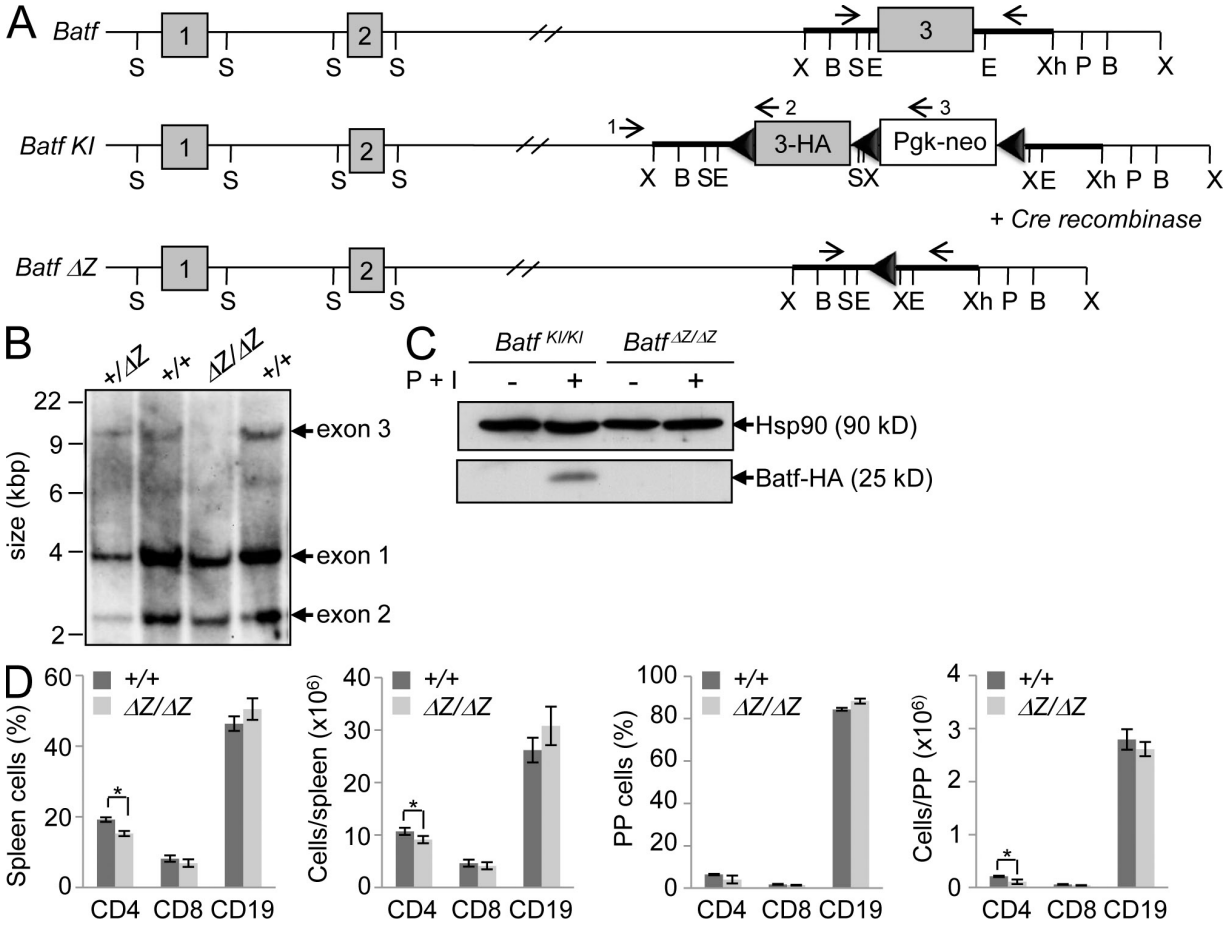

Figure 1. Profile of T and B cells in $Batf^{\Delta Z/\Delta Z}$ mice. (A) Schematic of *Batf KI* and *Batf* exon 3–deleted (*ΔZ*) alleles. *Batf* exons 1–3 are numbered. Filled triangles indicate loxP sites. Arrows indicate genotyping primers. Numbered arrows indicate primers used to identify targeted ES clones. S, SpeI; X, XbaI; E, EcoRI; B, BamHI; Xh, XhoI; P, PstI. (B) A representative DNA blot from five independent experiments detects homozygous deletion of *Batf* exon 3 in $Batf^{\Delta Z/\Delta Z}$ mice. (C) Splenocytes from $Batf^{KI/KI}$ and $Batf^{\Delta Z/\Delta Z}$ mice were stimulated with 2.5 ng/ml PMA and 125 ng/ml ionomycin (P + I) for 6 h. Cell extracts were immunoblotted using anti-HA mAb to detect Batf and anti–Hsp-90 mAb as a control for sample loading. A representative blot from three independent experiments is shown. (D) Cells from spleen and PP of $Batf^{+/+}$ and $Batf^{\Delta Z/\Delta Z}$ mice were analyzed by flow cytometry using anti-CD4 and anti-CD8 mAb to detect T cells and anti-CD19 mAb to detect B cells. The mean percentage of total cells of each set is shown on the left, and the mean cell number per spleen or per mouse PP is shown on the right. Data are means of three experiments performed with three mice per group ($n = 9$). Error bars indicate SE. *, $P < 0.05$.

Impaired Ig production in *Batf*$^{\Delta Z/\Delta Z}$ mice

IL-21 is required for the differentiation of Th17 cells and, in turn, is produced by Th17 cells (and other cells types) to stimulate IL-21–producing CD4$^+$ Tfh cells and the B cell Ab response (King, 2009). Mice lacking IL-4 and the IL-21 receptor exhibit severe defects in Ab production (Ozaki et al., 2002). To test if the combined IL-4– and IL-21– deficient phenotype of *Batf*$^{\Delta Z/\Delta Z}$ mice results in reduced Ig production, circulating IgM, IgG1, IgG2c, IgA, and IgE were quantified by ELISA. As shown in Fig. 3 A, when compared with *Batf*$^{+/+}$ animals, *Batf*$^{\Delta Z/\Delta Z}$ mice displayed a modest reduction in circulating IgM. Strikingly, the levels of all other Ig classes examined were barely detectable in *Batf*$^{\Delta Z/\Delta Z}$ mice.

To test if Ig production in *Batf*$^{\Delta Z/\Delta Z}$ mice remains low in the presence of antigen challenge, *Batf*$^{+/+}$ and *Batf*$^{\Delta Z/\Delta Z}$ mice were injected with sheep RBC (sRBC) or mock injected with PBS. After 7 d, serum was isolated and circulating Ig quantified by ELISA. Again, although anti-sRBC IgM was induced in both *Batf*$^{+/+}$ and *Batf*$^{\Delta Z/\Delta Z}$ mice, induction of IgG by *Batf*$^{\Delta Z/\Delta Z}$ mice was only 26% of the control (Fig. 3 B). Immunohistochemistry (IHC) confirmed the low levels of IgG1 and IgG2c in spleens of *Batf*$^{\Delta Z/\Delta Z}$

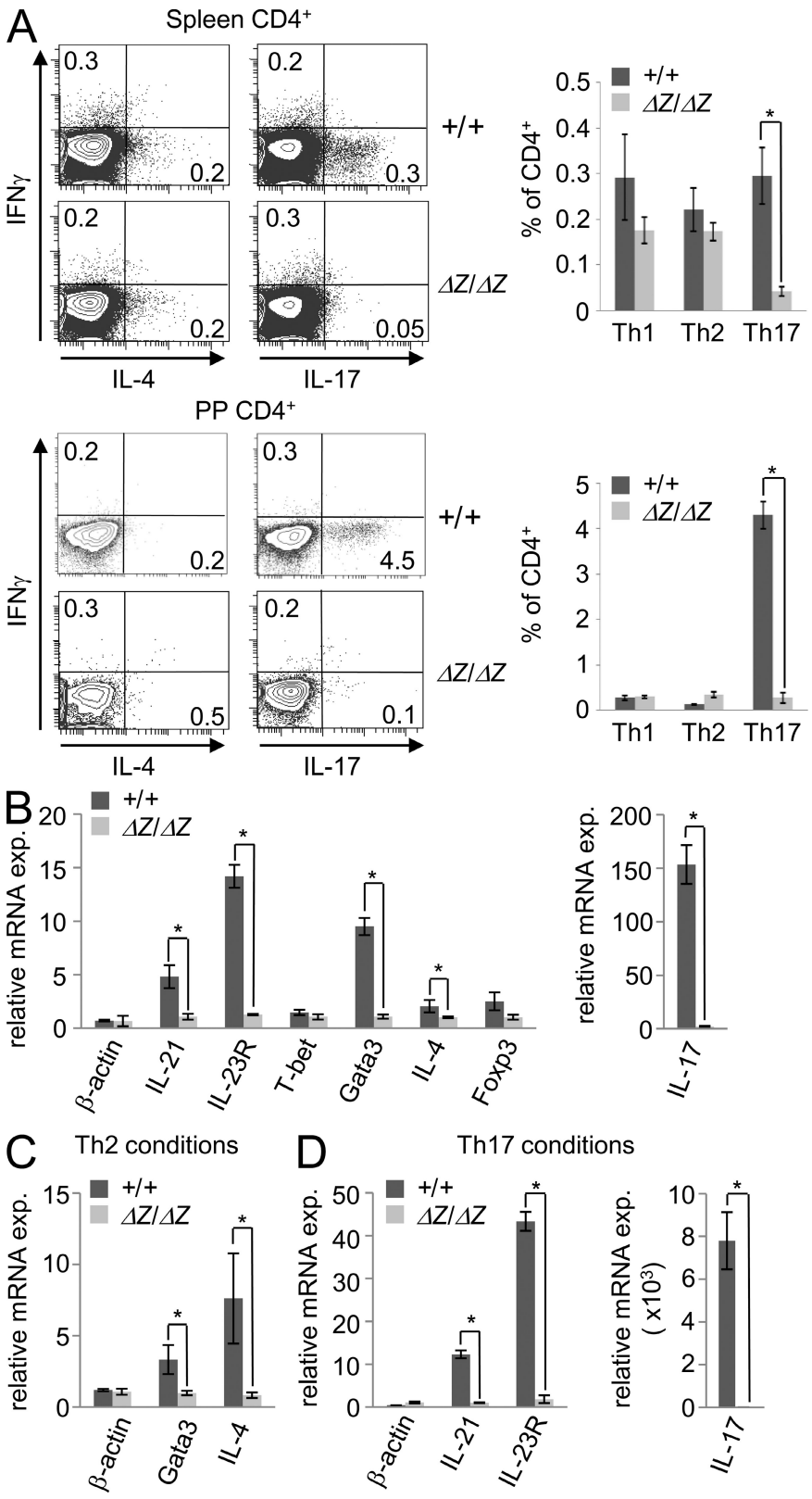

Figure 2. Th17 and Th2 differentiation is impaired in *Batf*$^{\Delta Z/\Delta Z}$ mice. (A) Cells from spleens and PP of *Batf*$^{\Delta Z/\Delta Z}$ and *Batf*$^{+/+}$ mice were surface stained using anti-CD4 mAb. After stimulation with 50 ng/ml P + 1 µg/ml I with 1 µg/ml monensin for 4 h, intracellular mAb staining was used detect IFN-γ–, IL-4–, and IL-17–expressing cells by flow cytometry. Representative flow plots are shown, along with the mean percentage of CD4$^+$ cells positive for each cytokine, calculated from two experiments with three mice per group ($n = 6$). Error bars indicate SE. *, $P < 0.05$. (B) CD4$^+$ cells from spleens of *Batf*$^{\Delta Z/\Delta Z}$ and *Batf*$^{+/+}$ mice ($n = 3$) were stimulated with anti-CD3ε mAb for 48 h. RNA was isolated, converted to cDNA, and assayed in duplicate for the indicated transcripts by qPCR. The mean relative mRNA expression is shown. Error bars indicate SE. *, $P < 0.05$. (C and D) Naive T cells from *Batf*$^{\Delta Z/\Delta Z}$ and *Batf*$^{+/+}$ spleens were cultured for 5–6 d with 5 µg/ml anti-CD3ε, 2 µg/ml anti-CD28, and 20 U/ml rhIL-2 and the following skewing conditions: Th2, 20 ng/ml rmIL-4, 10 µg/ml anti–IFN-γ mAb, and 10 µg/ml anti–IL-12 mAb; Th17 was described in Wang et al. (2009). Cytokine gene expression was detected by qPCR as in B. Data shown were averaged from five (Th2) and three (Th17) independent RNA preps assayed in duplicate. Error bars indicate SE. *, $P < 0.05$.

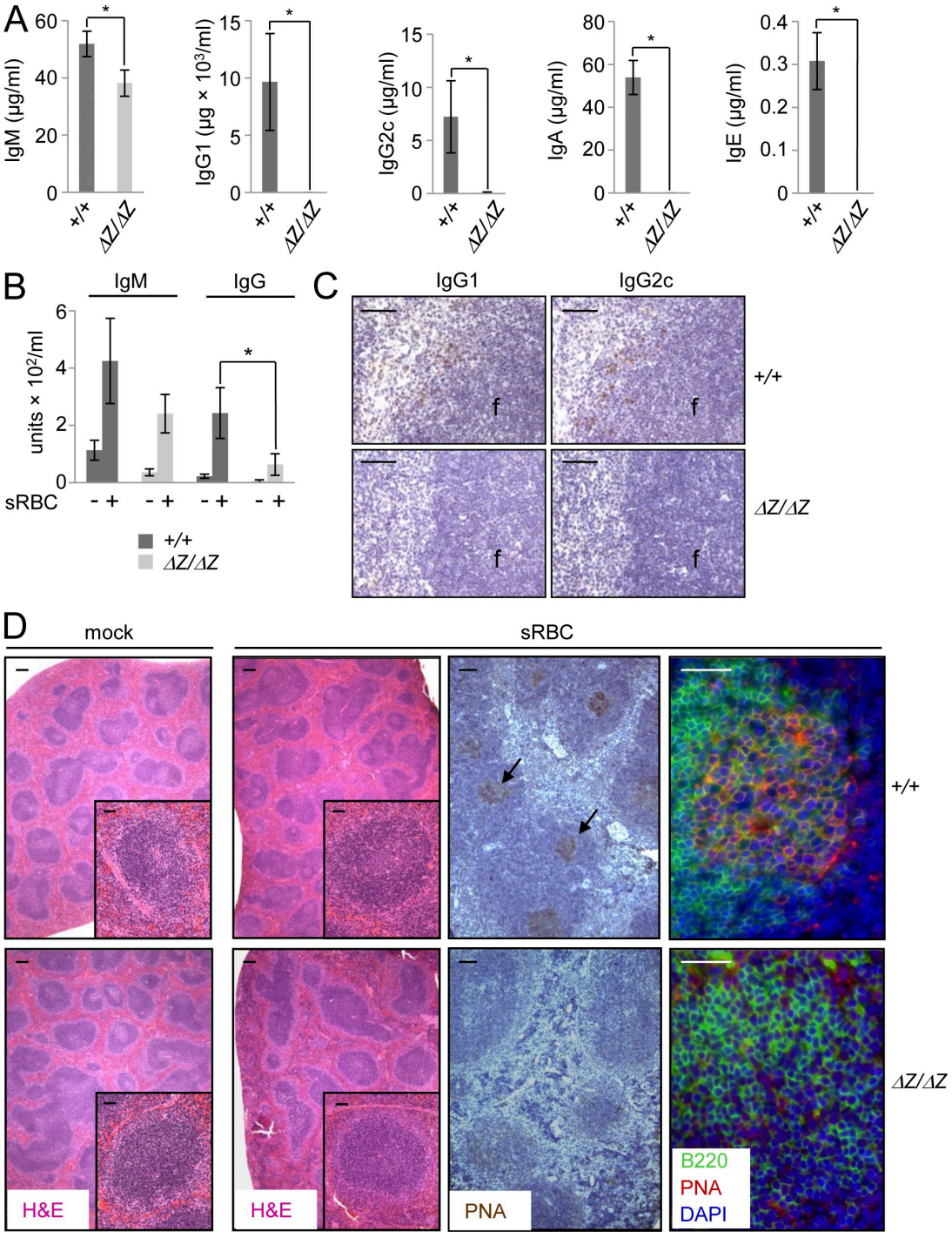

Figure 3. Dysgammaglobulinemia in *Batf*$^{\Delta Z/\Delta Z}$ mice. (A) ELISA was performed to measure the indicated Ig in sera of *Batf*$^{+/+}$ and *Batf*$^{\Delta Z/\Delta Z}$ mice. Shown are mean results from four mice per group ($n = 4$) assayed in duplicate. Error bars indicate SE. *, $P < 0.05$. (B) Sera from *Batf*$^{+/+}$ and *Batf*$^{\Delta Z/\Delta Z}$ mice, immunized with sRBC or mock injected with PBS, were used in ELISA to detect sRBC-specific IgM or IgG. Mean results from one ($n = 3$) of two experiments are shown. Error bars indicate SE. *, $P < 0.05$. (C) Spleen sections from mice in B ($n = 3$ for each genotype) were incubated with primary anti-IgG1 and anti-IgG2c Abs. Complexes were detected using biotinylated secondary Abs and Vectastain ABC reagent. Shown are representative images, counterstained with H (no E) and photographed at 40×. f, follicle. Bars, 50 µm. (D) Spleen sections from mice in B ($n = 3$ for each genotype) were stained with H + E (left) and photographed at 4× (bars, 250 µm) or 20× (insets; bars, 50 µm). GCs (arrows) were detected on additional sections (right) using biotinylated PNA and Vectastain ABC reagent, counterstained with H (no E; 20×; bars, 50 µm) or using biotinylated PNA, anti-mouse B220, DAPI, and fluorescently labeled secondary mAbs (60×; bars, 50 µm).

mice (Fig. 3 C). The morphology of additional spleen sections from sRBC-challenged *Batf*$^{+/+}$ and *Batf*$^{\Delta Z/\Delta Z}$ mice was examined (Fig. 3 D). Although hematoxylin and eosin (H + E) and peanut agglutinin (PNA) staining demonstrated the presence of GCs in *Batf*$^{+/+}$ mice, PNA^{+} GCs were conspicuously absent in *Batf*$^{\Delta Z/\Delta Z}$ mice.

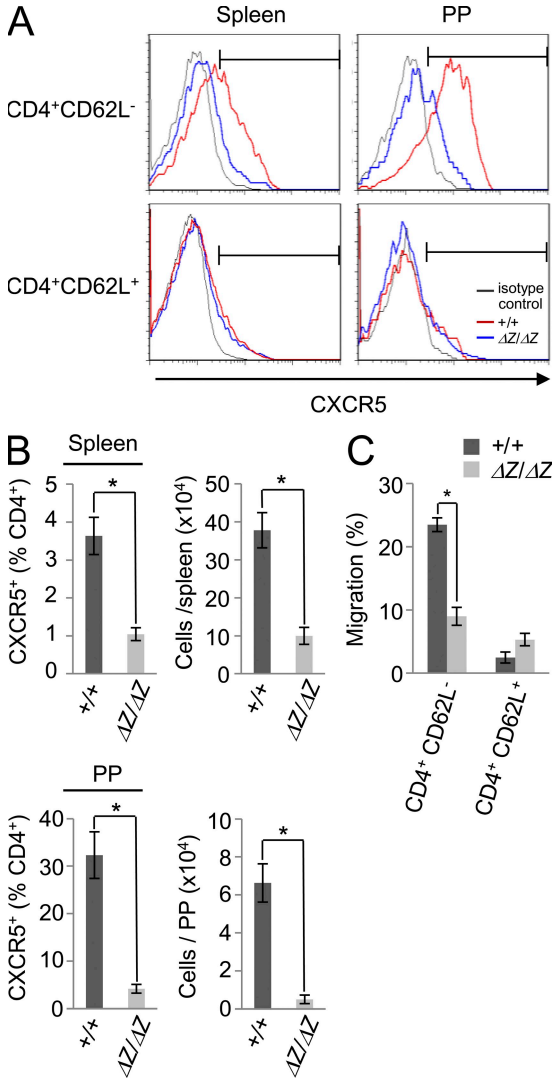

Figure 4. Dysfunctional Tfh cells in *Batf*$^{\Delta Z/\Delta Z}$ mice. (A) Cells from spleen and PP of *Batf*$^{\Delta Z/\Delta Z}$ and *Batf*$^{+/+}$ mice were stained with anti-CD4, anti-CD44, anti-CD62L, and anti-CXCR5 mAb (or isotype control) and Tfh cells detected by flow cytometry. Representative plots ($n = 9$) showing CXCR5 expression after gating on CD44^{+}CD4^{+}CD62L^{+} or CD44^{+}CD4^{+}CD62L^{-} cells are presented. (B) Datasets from A ($n = 9$) are plotted as the mean percentage of CD62L^{-}CXCR5^{+} of total CD4^{+} (left) or number of CXCR5^{+} cells per organ or per total mouse PP (right) with SE. *, $P < 0.05$. (C) 5×10^5 cells from PP were allowed to migrate to rmCXCL13 for 3 h. Migrated cells were stained with anti-CD4 and anti-CD62L mAbs and analyzed by flow cytometry. Migration is the number of migrating cells (+ ligand) minus the number migrating cells (no ligand) expressed as a percentage of CD4^{+}CD62L^{-} or CD4^{+}CD62L^{+} cells in the starting population. Mean results from three experiments are shown ($n = 3$). Error bars indicate SE. *, $P < 0.05$.

Reduced Tfh cell number and function in *Batf*$^{\Delta Z/\Delta Z}$ mice

The production of high-affinity class-switched Ab relies on GC interactions between B cells and Tfh cells (King, 2009). Tfh cells are characterized by the expression of CXCR5 (CXC chemokine receptor 5), which directs the homing of Tfh cells to B cell follicles in the spleen and lymph nodes (Kim et al., 2001). There is strong evidence to suggest that IL-21 is critical for Tfh development and that the IL-21 produced by Tfh cells in GCs is essential for the B cell response (Nurieva et al., 2008; Vogelzang et al., 2008; King, 2009). To quantify Tfh cells in *Batf*$^{+/+}$ and *Batf*$^{\Delta Z/\Delta Z}$ mice, CD4^{+} T cells were stained with mAb specific for CXCR5 and CD62L and analyzed by flow cytometry (Fig. 4 A). Results show that in *Batf*$^{\Delta Z/\Delta Z}$ mice, memory-type CD62L^{-}CXCR5^{+} Tfh cells are reduced by 70% in the spleen (Fig. 4 B, top) and by 90% in PP (Fig. 4 B, bottom). To examine if Tfh cells in *Batf*$^{\Delta Z/\Delta Z}$ mice are functional, purified CD4^{+} T cells from PP were challenged in vitro to migrate to CXCL13, the CXCR5 ligand. Migrating cells were counted and expressed as a percentage of CD62L^{-}CXCR5^{+} cells in the initial suspensions. As shown in Fig. 4 C, ~25% of *Batf*$^{+/+}$ Tfh cells were capable of chemotaxis, whereas <10% of *Batf*$^{\Delta Z/\Delta Z}$ Tfh cells displayed this behavior. These results are further support for an essential role for Batf in CXCR5^{+} Tfh cells.

Batf deletion has an impact on multiple CD4^{+} T cell lineages and, in doing so, generates an environment unfavorable to a robust Ab response. To demonstrate the T cell dependence of this phenotype, adoptive transfer was used to reconstitute T cell–deficient mice with CD4^{+} T cells purified from *Batf*$^{+/+}$ or *Batf*$^{\Delta Z/\Delta Z}$ mice. After transfer, the mice were challenged with sRBC and, 8 d later, Tfh cells were quantified and sera assayed for Ig. As predicted, when compared with mice reconstituted with *Batf*$^{+/+}$ T cells, the spleens and lymph nodes of mice reconstituted with *Batf*$^{\Delta Z/\Delta Z}$ T cells were not populated with CD62L^{-}CXCR5^{+} cells (Fig. 5, A and B) and sera from these animals contained less sRBC-induced IgM and IgG1 (Fig. 5 C).

Batf$^{\Delta Z/\Delta Z}$ B cells do not express *Aicda* mRNA and do not undergo CSR

To this point, our data implicate defects associated with several CD4^{+} T cell subsets as the underlying cause of Ig deficiency in *Batf*$^{\Delta Z/\Delta Z}$ mice. On the other hand, because Batf is expressed in mouse B cells (Williams et al., 2001) and functions as an inducible growth regulator in human B cells (Johansen et al., 2003), the loss of Batf could impact B cell function as well. To examine this possibility, resting B cells from spleens of *Batf*$^{+/+}$ and *Batf*$^{\Delta Z/\Delta Z}$ mice were cultured in control medium or in medium containing LPS, with or without added IL-4. Cells were analyzed for proliferation by BrdU staining after 40 h and for surface and secreted Ig after 4 d. *Batf*$^{+/+}$ and *Batf*$^{\Delta Z/\Delta Z}$ B cells proliferated similarly after exposure to LPS or LPS and IL-4 (Fig. 6 A). B cells of both genotypes also expressed surface and secreted IgM under all three growth conditions (Fig. 6 B). Strikingly, although control cells stimulated with LPS and IL-4 decreased

IgM production and began producing IgG1 and IgE, *Batf*$^{\Delta Z/\Delta Z}$ cells continued to produce high levels of IgM, indicating that Batf is required for efficient CSR.

The inability of *Batf*$^{\Delta Z/\Delta Z}$ B cells to undergo CSR after stimulation was characterized further using qPCR to examine the expression of key genes known to participate in events critical for B cell maturation and CSR (Honjo et al., 2004; Fairfax et al., 2008). As a first indication that Batf was regulated as a part of this process, we observed that *Batf* mRNA is induced by LPS in *Batf*$^{+/+}$ cells and was increased further by costimulation with IL-4 (Fig. 6 C). The absence of Batf did not dramatically affect the stimulation-induced down-regulation of *Pax5* or *Bcl-6* mRNA, nor did it prevent the up-regulation of *Irf4*, *Prdm1*, or *Xbp1s* mRNAs, although *Batf*$^{\Delta Z/\Delta Z}$ B cells did appear to resist IL-4–induced modulation of this latter group of transcripts. Interestingly, expression of the *Aicda* gene encoding AID (activation-induced cytidine deaminase) was undetectable in stimulated *Batf*$^{\Delta Z/\Delta Z}$ cells (Fig. 6 C). This finding is consistent with the lack of CSR and suggests that Batf participates in an essential molecular event downstream of B cell activation and upstream of *Aicda* expression, CSR, and somatic hypermutation (Fairfax et al., 2008; Park et al., 2009).

To confirm that this in vitro result reflects a B cell defect in vivo, *Batf*$^{+/+}$ and *Batf*$^{\Delta Z/\Delta Z}$ mice were injected with TNP-LPS. After 4 d, T cell–independent responses were assayed by ELISA and IHC. Although *Batf*$^{+/+}$ animals induced TNP-LPS–specific IgG1 (Fig. 6 D) and their spleens displayed foci of both IgG1- and IgG2c-producing B cells (Fig. 6 E), *Batf*$^{\Delta Z/\Delta Z}$ mice showed no T cell–independent antigen response by either assay.

The recent work of Schraml et al. (2009) clearly demonstrated a role for Batf in Th17 cell differentiation and cytokine gene regulation. Our studies have confirmed that role and have described additional roles for Batf in Tfh and Th2 cells that are required for the generation of a robust T cell–dependent antigen response in vivo. Moreover, our studies have revealed a role for Batf in the intrinsic responsiveness of B cells to T cell–independent stimulation in vitro and in vivo. Future studies, in which we exploit our conditional *Batf ΔZ* allele to disrupt Batf function in specific lymphocyte compartments or during key developmental transitions, will allow us to further dissect the molecular details of these intriguing Batf-dependent phenotypes.

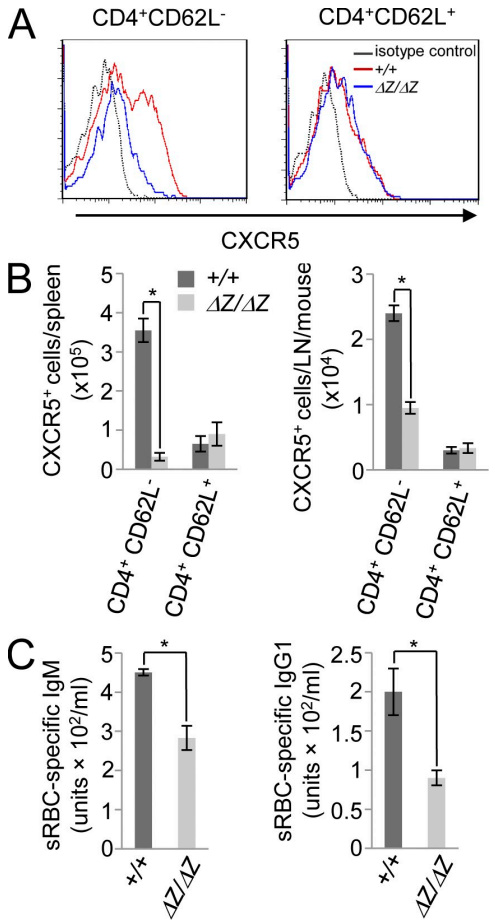

Figure 5. Limited response of *Batf*$^{\Delta Z/\Delta Z}$ CD4$^+$ T cells to T cell–dependent antigen. (A) CD4$^+$ T cells from *Batf*$^{+/+}$ or *Batf*$^{\Delta Z/\Delta Z}$ mice were injected into T cell–deficient mice, which were immunized with 5 × 10^8 sRBC. After 8 d, Tfh cells in spleen and lymph nodes were quantified as in Fig. 4 A. Representative plots (n = 3) are shown. (B) Mean number of CXCR5$^+$ cells from A per organ or per mouse lymph node (LN) is shown (n = 3). Error bars indicate SE. *, P < 0.05. (C) ELISA using sera isolated from mice in A to detect sRBC-specific IgM and IgG1. Mean and SE are shown (n = 3). *, P < 0.05.

MATERIALS AND METHODS

Generation of *Batf*$^{KI/KI}$ and *Batf*$^{\Delta Z/\Delta Z}$ mice. *Batf* primers with a 5′ loxP sequence and a 3′ HA epitope coding sequence (+ stop) were used to amplify a region of intron 2 plus exon 3 (− stop) of the *Batf* gene. This fragment was cloned into *pBS KS* and modified by insertion of the *Batf* 3′ UTR at SpeI and of a loxP-flanked *Pgk-neomycin* selection cassette at XbaI. The *Batf KI* sequence was excised using EcoRI and cloned into *pBS KS ARMS* containing 3.5 kbp of 5′ and 2.7 kbp of 3′ *Batf* genomic DNA. This plasmid, *pBS KS CKO*, was linearized and introduced into 129/SV mouse embryonic stem cells, and the correct targeting of drug-resistant clones was determined by PCR with forward (5′-GGACTAGTCATCTTGCCTT-3′) and reverse primers to detect endogenous (5′-GGAAGGCATGGGCACTCTATAC-3′) or recombined (5′-CGAGCATAGTGAGACGTGCTAC-3′) *Batf*. The Transgenic Mouse Core Facility of the Purdue University Center for Cancer Research produced germline chimeras which were crossed to C57BL/6 mice (Harlan). *Batf*$^{+/KI}$ mice were mated to produce *Batf*$^{KI/KI}$ mice which were crossed to *EIIaCre* mice (JAX). *Batf*$^{+/\Delta Z}$ mice were backcrossed to C57BL/6 mice four to six times and were mated to generate *Batf*$^{\Delta Z/\Delta Z}$ and littermate control *Batf*$^{+/\Delta Z}$ and *Batf*$^{+/+}$ mice that were used for experimentation at 7–12 wk of age. The genotyping primers for *Batf ΔZ* are forward, 5′-GCTTGTCTCTCACTAGTGAG-3′, and reverse, 5′-CTGTAGAGTGACTGGCTC-3′. All mice used in this study were maintained in a specific pathogen-free animal facility according to institutional guidelines. All animal protocols were reviewed and approved by the Purdue University Animal Care and Use Committee.

DNA blot hybridization. 20 µg DNA, isolated from tail tips by phenol/chloroform extraction, was digested with SpeI and resolved by 0.8% agarose gel electrophoresis. DNA was transferred to Zeta Probe membrane (Bio-Rad Laboratories), cross-linked, and probed using the *Batf* cDNA as previously described (Williams et al., 2001).

Immunoblot. Protein was isolated from stimulated splenocytes using RIPA buffer supplemented with protease inhibitors. Immunoblots to detect

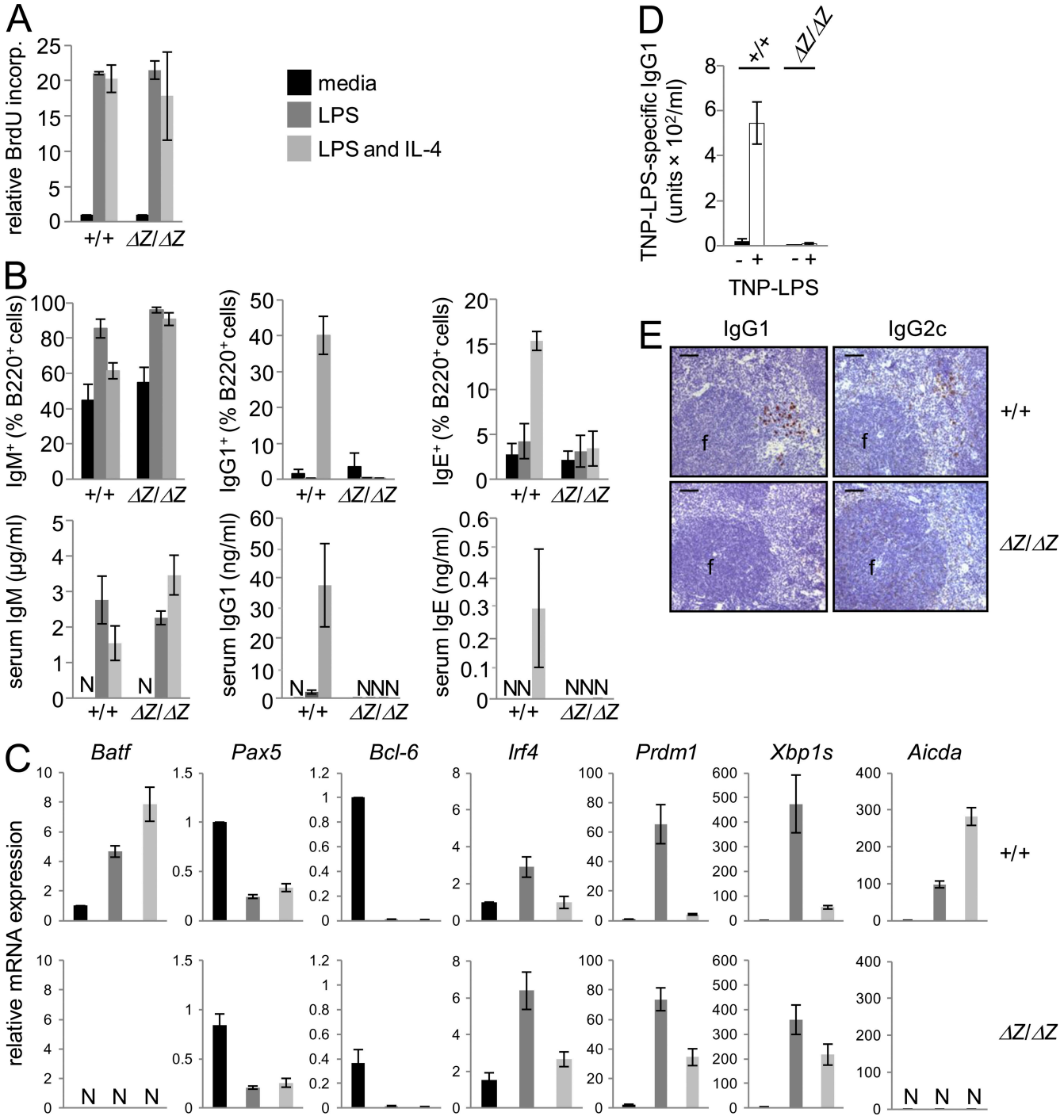

Figure 6. ***Batf*$^{\Delta Z/\Delta Z}$ B cells do not undergo CSR.** (A) B cells purified from *Batf*$^{+/+}$ and *Batf*$^{\Delta Z/\Delta Z}$ mice were cultured in media, or media supplemented with 20 µg/ml LPS, with or without 20 ng/ml IL-4. After 24 h, DNA synthesis was quantified by BrdU labeling for 16 h. Shown is mean BrdU incorporation, relative to *Batf*$^{+/+}$ or *Batf*$^{\Delta Z/\Delta Z}$ cells in media (set to 1.0), from three experiments (n = 3) performed in triplicate. Error bars indicate SE. (B) B cells cultured as in A were assayed for surface Ig expression by flow cytometry (top) and for secreted Ig by ELISA (bottom). The mean and SE were calculated from three experiments (n = 3). N, not detected. (C) RNA from cells in B was assayed for the indicated transcripts using qPCR. Data are averaged from three experiments (n = 3) performed in triplicate and expressed relative to the *Batf*$^{+/+}$ media control (set to 1.0). Error bars indicate SE. N, not detected. (D) Sera from *Batf*$^{+/+}$ and *Batf*$^{\Delta Z/\Delta Z}$ mice immunized with TNP-LPS or PBS were analyzed by ELISA for TNP-specific IgG1. Mean results from three mice per group (n = 3) are plotted. Error bars indicate SE. (E) Spleen sections from mice in D (n = 3 for each genotype) were stained as in Fig. 3 C to detect IgG1- and IgG2c-producing cells. Representative images are shown (20×). f, follicle. Bars, 50 µm.

Batf-HA and control of Hsp90 proteins were performed as previously described (Thornton et al. 2006; Zhu et al. 2007).

Flow cytometry. Flow cytometry was performed using an FC500 (Beckman Coulter) or Canto II (BD) cytometer and data analyzed using FCSExpress3 (De Novo Software). Fc block prevented nonspecific Ab interactions. mAbs used are indicated in the figure legends. The identity and source of all Abs are listed in Table S2. Intracellular staining to detect $CD4^+$ T cells reactive with IFN-γ, IL-4, and IL-17A mAbs was performed as previously described (Wang et al., 2009).

Cell culture. Splenocytes were prepared and $CD4^+$ T and resting B cells isolated using CD4 (L3T4) and CD43 magnetic bead separation, respectively (Miltenyi Biotec). Cells were cultured as previously described (Snapper et al., 1988; Williams et al., 2003). Stimulations and in vitro skewing conditions are detailed in figure legends. B cell proliferation was measured using a BrdU cell proliferation kit (Millipore).

Analysis of RNA. Semi-qPCR was performed as previously described (Thornton et al., 2006) and qPCR was performed with SYBR green (Roche) and a real-time PCR system (7300; Applied Biosystems). Primers are listed in figure legends or Table S1. Results were normalized to *Hprt* or *β-actin* expression. ΔΔCt values were used to calculate relative expression of each mRNA.

ELISA. Blood, collected by cardiac puncture, was allowed to clot at room temperature in a Microtainer Serum Separator tube (BD). Serum was isolated by centrifugation. ELISA for IgG2c and IgE was performed using OptEIA kits (BD). ELISA for IgG1, IgA, and IgM used mAb indicated in Table S2. Serum was diluted in Assay Diluent (BD) and applied to Ab-coated 96-well MaxiSorp plates (Nunc), and reactions were visualized with streptavidin-HRP and TMB substrate reagent (BD). ELISA plates and protocols for detecting sRBC-specific IgM and IgG were obtained from Life Diagnostics and IgG1 was obtained from Southern Biotech. ELISA to detect TNP-LPS–specific IgG1 used plates coated with 10 μg/ml TNP-BSA (Biosearch Technologies).

In vivo antigen stimulation and IHC. For T cell–dependent response, mice were injected i.p. with 5×10^8 sRBC in 200 μl PBS or PBS alone (mock). On day 8, sera were isolated for ELISA and spleen tissue was processed for IHC as previously described (Zhu et al., 2007). For T cell–independent response, mice were injected with 30 μg TNP-LPS (Sigma-Aldrich) or an equal volume of PBS. On day 5, sera were isolated for ELISA and spleen tissue was processed for IHC. GCs were detected using biotinylated PNA (1:300) and visualized with RTU Vectastain, ABC reagent, and DAB peroxidase substrate (Vector Laboratories). For fluorescent detection, antigens were retrieved by boiling in citrate buffer (Vector Laboratories) and sections blocked using anti–mouse IgG and an avidin/biotin blocking kit (Vector Laboratories). B cells were detected using rat anti–mouse CD45R (B220; 1:200) and FITC rabbit anti–rat IgG (1:200). GC B cells were identified using biotinylated PNA (1:100) and Texas Red conjugated avidin (Vector Laboratories; 1:200). Nuclei were stained with DAPI (Santa Cruz Biotechnology, Inc.). Ig-producing cells were detected using anti-IgG1 (1:400) or anti-IgG2c (1:200), a biotin rabbit anti–goat (1:200) Ab, and a NovaRed alkaline phosphatase substrate kit (Vector Laboratories).

Adoptive transfer and immunization. On day 0, 5×10^6 $CD4^+$ T cells from $Batf^{+/+}$ or $Batf^{\Delta Z/\Delta Z}$ mice were injected i.v. into T cell–deficient mice (B6.129P2-*Tcrb*^{tm1Mom} *Tcrd*^{tm1Mom}/J; JAX) and animals immunized i.p. with 5×10^8 sRBC in 100 μl PBS. Mice were sacrificed on day 8 for the analysis of T cell subsets and Ig production.

Chemotaxis assay. Chemotaxis assays were performed and analyzed as described previously (Lim et al., 2004). In brief, 5×10^5 lymphocytes from PP were added to the upper chamber of Transwell inserts (Corning) and allowed to migrate to media in a lower chamber containing 2.5 μg/ml rm-CXCL13. After 3 h, cells were collected and analyzed by flow cytometry.

Online supplemental material. Fig. S1 shows the expression of the mouse *Batf* gene in $Batf^{+/+}$, $Batf^{KI/KI}$, and $Batf^{\Delta Z/\Delta Z}$ mice. Fig. S2 compares the thymic T cell profile, the T reg cell profile, and the in vitro T reg, Th1, and Th17 differentiation profiles of $Batf^{+/+}$ and $Batf^{\Delta Z/\Delta Z}$ mice. Table S1 contains sequences of the oligonucleotide primers used in this study. Table S2 provides information on the antibodies used in this study. Online supplemental material is available at http://www.jem.org/cgi/content/full/jem.20091548/DC1.

The authors thank J.P. Robinson, K. Ragheb, C. Holdman, and the Purdue University Cytometry Laboratory for assistance with flow cytometry and S. Konieczny, J. Hallett, A. Kaufman, and the Transgenic Mouse Core Facility of the Purdue University Center for Cancer Research for the generation of *Batf KI* mice. Special thanks are extended to K. Williams and A. Zullo, whose Ph.D. thesis research provided a foundation for this work.

This study was supported by National Institutes of Health grants CA782464 and CA114381 (E. Taparowsky) and National Institutes of Health grant AI074745 (C.H. Kim). Predoctoral student support was provided by National Institutes of Health grant T32 GM08298 (K.L. Jordan-Williams and M.R. Logan) and by a Career Development Award from the Indiana CTSI (National Institutes of Health grant 5TL1 RR025759 to M.R. Logan).

The authors have no conflicting financial interests.

Submitted: 17 July 2009
Accepted: 23 March 2010

REFERENCES

Amoutzias, G.D., E. Bornberg-Bauer, S.G. Oliver, and D.L. Robertson. 2006. Reduction/oxidation-phosphorylation control of DNA binding in the bZIP dimerization network. *BMC Genomics*. 7:107–117. doi:10.1186/1471-2164-7-107

Aronheim, A., E. Zandi, H. Hennemann, S.J. Elledge, and M. Karin. 1997. Isolation of an AP-1 repressor by a novel method for detecting protein-protein interactions. *Mol. Cell. Biol.* 17:3094–3102.

Dorsey, M.J., H.J. Tae, K.G. Sollenberger, N.T. Mascarenhas, L.M. Johansen, and E.J. Taparowsky. 1995. B-ATF: a novel human bZIP protein that associates with members of the AP-1 transcription factor family. *Oncogene*. 11:2255–2265.

Echlin, D.R., H.J. Tae, N. Mitin, and E.J. Taparowsky. 2000. B-ATF functions as a negative regulator of AP-1 mediated transcription and blocks cellular transformation by Ras and Fos. *Oncogene*. 19:1752–1763. doi:10.1038/sj.onc.1203491

Eferl, R., and E.F. Wagner. 2003. AP-1: a double-edged sword in tumorigenesis. *Nat. Rev. Cancer*. 3:859–868. doi:10.1038/nrc1209

Fairfax, K.A., A. Kallies, S.L. Nutt, and D.M. Tarlinton. 2008. Plasma cell development: from B-cell subsets to long-term survival niches. *Semin. Immunol.* 20:49–58. doi:10.1016/j.smim.2007.12.002

Hess, J., P. Angel, and M. Schorpp-Kistner. 2004. AP-1 subunits: quarrel and harmony among siblings. *J. Cell Sci.* 117:5965–5973. doi:10.1242/jcs.01589

Hildner, K., B.T. Edelson, W.E. Purtha, M. Diamond, H. Matsushita, M. Kohyama, B. Calderon, B.U. Schraml, E.R. Unanue, M.S. Diamond, et al. 2008. Batf3 deficiency reveals a critical role for CD8alpha+ dendritic cells in cytotoxic T cell immunity. *Science*. 322:1097–1100. doi:10.1126/science.1164206

Honjo, T., M. Muramatsu, and S. Fagarasan. 2004. AID: how does it aid antibody diversity? *Immunity*. 20:659–668. doi:10.1016/j.immuni.2004.05.011

Iacobelli, M., W. Wachsman, and K.L. McGuire. 2000. Repression of IL-2 promoter activity by the novel basic leucine zipper $p21^{SNFT}$ protein. *J. Immunol.* 165:860–868.

Johansen, L.M., C.D. Deppmann, K.D. Erickson, W.F. Coffin III, T.M. Thornton, S.E. Humphrey, J.M. Martin, and E.J. Taparowsky. 2003. EBNA2 and activated Notch induce expression of BATF. *J. Virol.* 77:6029–6040. doi:10.1128/JVI.77.10.6029-6040.2003

Jung, M., R. Sabat, J. Krätzschmar, H. Seidel, K. Wolk, C. Schönbein, S. Schütt, M. Friedrich, W.D. Döcke, K. Asadullah, et al. 2004. Expression profiling of IL-10-regulated genes in human monocytes and

peripheral blood mononuclear cells from psoriatic patients during IL-10 therapy. *Eur. J. Immunol.* 34:481–493. doi:10.1002/eji.200324323

Kim, C.H., L.S. Rott, I. Clark-Lewis, D.J. Campbell, L. Wu, and E.C. Butcher. 2001. Subspecialization of CXCR5$^+$ T cells: B helper activity is focused in a germinal center–localized subset of CXCR5$^+$ T cells. *J. Exp. Med.* 193:1373–1381. doi:10.1084/jem.193.12.1373

King, C. 2009. New insights into the differentiation and function of T follicular helper cells. *Nat. Rev. Immunol.* 9:757–766. doi:10.1038/nri2644

Kronenberg, M., and I. Engel. 2007. On the road: progress in finding the unique pathway of invariant NKT cell differentiation. *Curr. Opin. Immunol.* 19:186–193. doi:10.1016/j.coi.2007.02.009

Li, J., G.W. Peet, D. Balzarano, X. Li, P. Massa, R.W. Barton, and K.B. Marcu. 2001. Novel NEMO/IkappaB kinase and NF-kappa B target genes at the pre-B to immature B cell transition. *J. Biol. Chem.* 276:18579–18590. doi:10.1074/jbc.M100846200

Lim, H.W., P. Hillsamer, and C.H. Kim. 2004. Regulatory T cells can migrate to follicles upon T cell activation and suppress GC-Th cells and GC-Th cell-driven B cell responses. *J. Clin. Invest.* 114:1640–1649.

Lim, J., T. Hao, C. Shaw, A.J. Patel, G. Szabó, J.F. Rual, C.J. Fisk, N. Li, A. Smolyar, D.E. Hill, et al. 2006. A protein-protein interaction network for human inherited ataxias and disorders of Purkinje cell degeneration. *Cell.* 125:801–814. doi:10.1016/j.cell.2006.03.032

Nurieva, R.I., Y. Chung, D. Hwang, X.O. Yang, H.S. Kang, L. Ma, Y.H. Wang, S.S. Watowich, A.M. Jetten, Q. Tian, and C. Dong. 2008. Generation of T follicular helper cells is mediated by interleukin-21 but independent of T helper 1, 2, or 17 cell lineages. *Immunity.* 29:138–149. doi:10.1016/j.immuni.2008.05.009

Ozaki, K., R. Spolski, C.G. Feng, C.F. Qi, J. Cheng, A. Sher, H.C. Morse III, C. Liu, P.L. Schwartzberg, and W.J. Leonard. 2002. A critical role for IL-21 in regulating immunoglobulin production. *Science.* 298:1630–1634. doi:10.1126/science.1077002

Park, S.R., H. Zan, Z. Pal, J. Zhang, A. Al-Qahtani, E.J. Pone, Z. Xu, T. Mai, and P. Casali. 2009. HoxC4 binds to the promoter of the cytidine deaminase AID gene to induce AID expression, class-switch DNA recombination and somatic hypermutation. *Nat. Immunol.* 10:540–550. doi:10.1038/ni.1725

Raivich, G., and A. Behrens. 2006. Role of the AP-1 transcription factor c-Jun in developing, adult and injured brain. *Prog. Neurobiol.* 78:347–363. doi:10.1016/j.pneurobio.2006.03.006

Rincón, M., and R.A. Flavell. 1996. Regulation of AP-1 and NFAT transcription factors during thymic selection of T cells. *Mol. Cell. Biol.* 16:1074–1084.

Schraml, B.U., K. Hildner, W. Ise, W.L. Lee, W.A. Smith, B. Solomon, G. Sahota, J. Sim, R. Mukasa, S. Cemerski, et al. 2009. The AP-1 transcription factor Batf controls T(H)17 differentiation. *Nature.* 460:405–409.

Senga, T., T. Iwamoto, S.E. Humphrey, T. Yokota, E.J. Taparowsky, and M. Hamaguchi. 2002. Stat3-dependent induction of BATF in M1 mouse myeloid leukemia cells. *Oncogene.* 21:8186–8191. doi:10.1038/sj.onc.1205918

Snapper, C.M., F.D. Finkelman, D. Stefany, D.H. Conrad, and W.E. Paul. 1988. IL-4 induces co-expression of intrinsic membrane IgG1 and IgE by murine B cells stimulated with lipopolysaccharide. *J. Immunol.* 141:489–498.

Su, Z.Z., S.G. Lee, L. Emdad, I.V. Lebdeva, P. Gupta, K. Valerie, D. Sarkar, and P.B. Fisher. 2008. Cloning and characterization of SARI (suppressor of AP-1, regulated by IFN). *Proc. Natl. Acad. Sci. USA.* 105:20906–20911. doi:10.1073/pnas.0807975106

Thornton, T.M., A.J. Zullo, K.L. Williams, and E.J. Taparowsky. 2006. Direct manipulation of activator protein-1 controls thymocyte proliferation *in vitro*. *Eur. J. Immunol.* 36:160–169. doi:10.1002/eji.200535215

Vogelzang, A., H.M. McGuire, D. Yu, J. Sprent, C.R. Mackay, and C. King. 2008. A fundamental role for interleukin-21 in the generation of T follicular helper cells. *Immunity.* 29:127–137. doi:10.1016/j.immuni.2008.06.001

Wagner, E.F., and R. Eferl. 2005. Fos/AP-1 proteins in bone and the immune system. *Immunol. Rev.* 208:126–140. doi:10.1111/j.0105-2896.2005.00332.x

Wang, C., S.G. Kang, J. Lee, Z. Sun, and C.H. Kim. 2009. The roles of CCR6 in migration of Th17 cells and regulation of effector T-cell balance in the gut. *Mucosal Immunol.* 2:173–183. doi:10.1038/mi.2008.84

Williams, K.L., I. Nanda, G.E. Lyons, C.T. Kuo, M. Schmid, J.M. Leiden, M.H. Kaplan, and E.J. Taparowsky. 2001. Characterization of murine BATF: a negative regulator of activator protein-1 activity in the thymus. *Eur. J. Immunol.* 31:1620–1627. doi:10.1002/1521-4141(200105)31:5<1620::AID-IMMU1620>3.0.CO;2-3

Williams, K.L., A.J. Zullo, M.H. Kaplan, R.R. Brutkiewicz, C.D. Deppmann, C. Vinson, and E.J. Taparowsky. 2003. BATF transgenic mice reveal a role for activator protein-1 in NKT cell development. *J. Immunol.* 170:2417–2426.

Zhou, L., M.M. Chong, and D.R. Littman. 2009. Plasticity of CD4+ T cell lineage differentiation. *Immunity.* 30:646–655. doi:10.1016/j.immuni.2009.05.001

Zhu, L., G. Shi, C.M. Schmidt, R.H. Hruban, and S.F. Konieczny. 2007. Acinar cells contribute to the molecular heterogeneity of pancreatic intraepithelial neoplasia. *Am. J. Pathol.* 171:263–273. doi:10.2353/ajpath.2007.061176

Zullo, A.J., K. Benlagha, A. Bendelac, and E.J. Taparowsky. 2007. Sensitivity of NK1.1-negative NKT cells to transgenic BATF defines a role for activator protein-1 in the expansion and maturation of immature NKT cells in the thymus. *J. Immunol.* 178:58–66.